DOI: 10.1021/ma100633y

Macromolecules
ARTICLE

Toughening Polypropylene and Its Nanocomposites with Submicrometer Voids

Aravind Dasari,*,†,‡ Qing-Xin Zhang,§ Zhong-Zhen Yu,*,†,⊥ and Yiu-Wing Mai†

†*Center for Advanced Materials Technology (CAMT), School of Aerospace, Mechanical and Mechatronic Engineering (Bldg. J07), University of Sydney, Sydney, NSW 2006, Australia,* ‡*Madrid Institute for Advanced Studies of Materials (IMDEA Materials), C/Profesor Aranguren s/n, 28040 Madrid, Spain,* §*Institute of Polymer Science and Engineering, School of Chemical Engineering and Technology,Hebei University of Technology, Tianjin 300130, China, and* ⊥*Department of Polymer Engineering, College of Materials Science and Engineering, Beijing University of Chemical Technology, Beijing 100029, China*

Received March 24, 2010; Revised Manuscript Received May 18, 2010

ABSTRACT: This paper deals with a novel concept of induction of well-distributed submicrometer voids in polypropylene (PP) and PP/$CaCO_3$ nanocomposites during processing to alleviate their brittleness without sacrificing Young's modulus and yield strength. The role of these voids in initiating/participating in the plastic deformation processes during tensile and double-notch four-point-bend (DN-4-PB) tests is investigated. It is shown that the voids act in a similar way as the cavitated rubber particles in rubber-toughened polymer systems; that is, plastic growth (of the pre-existent voids) in the PP matrix occurs upon deformation and subsequently triggers large plastic deformation of the surrounding matrix in the form of isolated and domainlike craze structures.

1. Introduction

In general, the addition of rigid particles to polymers improves their stiffness and strength, but the toughness results are rather mixed. In the majority of these studies, dramatic drops in fracture toughness compared to their corresponding pristine polymers are often noted. Only a few studies have reported increased toughness as well as elastic stiffness and strength.[1−4] Additionally, the extent of toughness enhancement, if at all, is not always significant. But the conventional approach of adding soft elastomer particles to combat inherent brittleness of many polymers suffers from a well-known drawback of reduced overall stiffness/strength. Nonetheless, the use of soft (or rigid) particles as tougheners is based on the concept that the particles must cavitate (or debond at the interface) and release the high plastic constraint in the matrix. Physically, the phenomena of particle−matrix interface debonding in a rigid particle/polymer system and rubber particle cavitation in a soft particle/polymer system effectively yield a void/polymer system. Thus, this has led to an idea of induction of submicrometer voids in polymers and examine their role in the fracture and deformation processes in order to (a) elucidate the importance of cavitation of rubber particles in toughening polymers[5−7] and/or (b) model and predict patterns of matrix deformation of rubber-filled polymers (where the rubber phase is assumed to be cavitated).[8]

Bagheri and Pearson[5−7] conducted a comparative examination of epoxies modified with various rubber particles having different cavitation resistance and pre-existing microvoids (hollow spheres up to 40 μm). They showed that the toughening efficiency was similar in both cases (rubber particles and microvoids), inducing shear yielding at the crack tip. However, their influence on yield stress of the blend was different; at a given size and concentration, epoxies containing microvoids had relatively higher yield stress than rubber-modified materials. Guild and Young[9] performed finite element analysis of the stress distributions in the matrix for epoxy-containing rubber particles (spheres) and compared to epoxy-containing microvoids. They found that the stress distributions were very similar in both cases. But Fukui et al.,[10] from their elastic−plastic finite element analysis on ethylene-*co*-propylene rubber-modified polyamide 6 using a two-dimensional model, suggested that rubber particles provided a more favorable situation for toughening than microvoids, since the latter could cause cracking in the matrix. Nonetheless, cracking was observed in the experimental study of Bagheri and Pearson[5] with epoxies only when the void size was ~40 μm, suggesting that if the pre-existing voids are even smaller, they might enhance fracture toughness without causing degradation of other properties. Lazzeri and Bucknall[11] also proposed that rubber particles may be distinguished from microvoids at later stages of deformation, when they contribute to strain hardening of the ligament and postpone its failure; i.e., when the polymer ligaments are very thin, rubber particles are more effective tougheners than pre-existing voids since they can suppress the failure of the ligaments. Huang and Kinloch[12] used urea-terminated polyether amine as a microvoiding agent in epoxy and created voids of ~0.70 μm. This voided material exhibited improved fracture toughness (K_{Ic} ~ 1.96 MPa $m^{1/2}$) compared to neat epoxy (K_{Ic} ~ 1.03 MPa $m^{1/2}$) without voids although the toughening mechanisms were not studied.

With this background, in the present study we manufactured the concept of induction of submicrometer voids, for the first time, in a thermoplastic, polypropylene (PP), and its nanocomposites to initiate a tough response without degrading stiffness/strength. Polyoxyethylene nonylphenol (PN) was employed to obtain submicrometer voids in PP with and without calcium carbonate ($CaCO_3$) particles. PN is a nonionic surfactant with a hydrophobic hydrocarbon end and a hydrophilic hydroxyl end and is traditionally used as a dispersing agent for nanoparticles or as an antistatic agent in polymers and textiles industries.

2. Experimental Work

2.1. Materials and Preparation. PP was supplied by ICI Australia Operations under a trade name of GWM 22. The melt

*Corresponding authors: e-mail aravind.dasari@imdea.org, Fax +34-91-550 3047 (A.D.); e-mail yuzz@mail.buct.edu.cn, Fax +86-10-6442 8582 (Z.-Z.Y.).

 Published on Web 06/02/2010

flow index and density provided by the supplier are 4.4 g/10 min and 0.905 g/cm^3, respectively. Guang Ping Nano Technology Group (Hong Kong) provided the spherical $CaCO_3$ nanoparticles (trade name CCR) with an average diameter of 44 nm. PN was obtained from Tianjin Feejy Trade Corp. Ltd. (China) with a hydrophilic hydroxyl end [$-(OC_2H_4)_{10}OH$] and a hydrophobic hydrocarbon end [$-C_9H_{19}$]. PN modifier (0.75, 1.50, and 2.25 phr) and/or $CaCO_3$ particles (5, 10, 15, and 20 wt %) were added to the PP pellets by dry mixing prior to melt extrusion in a corotating Werner and Pfleider ZSK-30 twin-screw extruder. The extruder was operated at temperatures of 190−200 °C and a screw speed of 300 rpm. The extrudates were pelletized at the die exit, dried, and then injection-molded (BOY 22s dipronic machine) into standard tensile and rectangular bars. The barrel and mold temperatures were maintained at 200 and 60 °C, respectively.

2.2. Morphology Observations and Quantification. To investigate the size and distribution of voids formed due to the addition of PN, freeze-fractured surfaces were observed with a Philips S-505 scanning electron microscope (SEM) from surface to midthickness regions, and then the morphology was quantified using image analysis (Image J). To study the dispersion of $CaCO_3$ particles, ultrathin sections from the mid cross-section regions of the samples, ranging from 60 to 90 nm, were cryogenically cut with a diamond knife at −80 °C using a Leica Ultracut S microtome and collected on holey Formvar/carbon-coated 400-mesh copper grids. Sections were then observed with a Philips CM12 transmission electron microscope (TEM) at an accelerating voltage of 120 kV.

2.3. Mechanical Testing. Standard tensile tests were conducted on dumbbell-shaped specimens with an Instron 5567 tensile tester at a crosshead speed of 50 mm/min and to different selected extensions in ambient conditions. An extensometer was used for determining the longitudinal strain (or extension). The gauge length used for the purpose was 50 mm. Notched Izod impact strength (J/m) was evaluated in an ITR-2000 instrumented impact tester according to ASTM D256 on the standard sized rectangular bars having a 45° V-notch (depth of 2.54 mm) machined midway on one side of the bar. Further, the DN-4-PB technique was used to investigate the deformation history of the materials in the vicinity of the crack tip. Injection-molded rectangular specimens were given two sharp identical notches using a razor blade. The distance between the two sharp notches on the DN-4-PB bar was set at 10 mm to ensure that the two cracks propagated independently. The specimens were then tested using the Instron 5567 machine at a crosshead speed of 1 mm/min. A plastic zone is independently formed at each crack tip due to stress intensification. After one notch fails, the other is still in a subcritical condition with a damaged zone. At least five samples were tested in all the tests conducted.

2.4. Deformation Mechanisms. To understand the role of submicrometer voids in the toughening processes, ultrathin sections were obtained from selected regions along the tensile stretched specimens and from the damage zone in the DN-4-PB test. Subsequently, they were observed in TEM. Additionally, the damage zone of the unbroken notch tip in the DN-4-PB test was observed using a LEITZ DMRXE transmission optical microscope after obtaining thin sections (~25 μm).

3. Results and Discussion

3.1. Morphological Characterization. SEM micrographs of the freeze-fractured PP/PN blends in the core (midthickness), midway between the core and the surface (intermediate), and in proximity to the surface of injection molded bar with a selected PN content of 1.50 phr are shown in Figure 1a. Well-dispersed submicrometer voids are evident in the blend; these are formed as a result of the addition of PN to PP matrix as no voids were observed in neat PP (not shown here). The formation of voids can be attributed to the low flash point of PN (~90 °C), which is well below the processing temperature (~200 °C) of PP, thus resulting in vapor or bubble formation during processing. During the travel process of the bubbles from the melt into the ambient, they break, resulting in the large size voids in the core, medium size voids with increased number in the midregion between the core and the surface (intermediate), and small size voids in the proximity of the surface with a large number (Figure 1b). PP/PN blends with 0.75 and 2.25 phr PN also exhibited voids in a similar sequence. The average values of the size and density in different regions in all samples with different PN content are given in Table 1, which clearly show that with increasing amounts of PN void size increases in similar locations.

Similarly, in PP/$CaCO_3$ systems, the presence of PN resulted in the induction of submicrometer voids. But compared to PP/PN systems and at a given amount of PN, voids in PP/PN/$CaCO_3$ systems are relatively larger. This may be due to the obstructions ($CaCO_3$) in the path of moving bubbles. Average void size distributions for 15 wt % of $CaCO_3$ are listed in Table 1. Besides the formation of voids, the presence of PN surfactant in PP/$CaCO_3$ system, as expected, improved dispersion/distribution of $CaCO_3$ (micrographs not shown here).

3.2. Mechanical Properties. Figure 2a shows that the addition of PN in small concentrations does not significantly alter the Young's modulus and yield strength of PP. The slight reductions can be due to the plasticization effect of the PN. It is also worth noting that the decrease in Young's modulus and yield strength is nominal compared to rubber-toughened polymer systems where a significant drop is generally expected.[13] Interestingly, notched Izod impact strength is almost doubled with the addition of PN (Figure 2b), pointing to a beneficial aspect of pre-existent submicrometer voids.

As expected with all polymer/$CaCO_3$ systems, modulus increased noticeably (though not dramatically) and yield strength decreased slightly with particle loading (Figure 3a,b); for example, modulus increased from ~0.70 GPa (neat PP) to ~0.8 GPa (15 wt % $CaCO_3$), while yield strength decreased from ~34.7 MPa to ~30.7 MPa for the respective materials. The slight improvements/degradations in modulus/yield strength were observed in many other studies[4,14,15] and can be attributed to the poor interaction of particles with the matrix (leading to their easy/early debonding). Even in the additional presence of PN, similar trends were observed. It is interesting to note that the ratios of decrease in modulus for PP and PP/PN systems to PP/$CaCO_3$ and PP/PN/$CaCO_3$ systems are very similar. This indicates that the PN is contributing independently to the systems. This is also evident in the notched impact strength data shown in Figure 3c, which demonstrates independent individual contributions of PN and $CaCO_3$. The mechanisms of this property improvement are discussed below.

It is also important to confirm if there are any changes in the crystal structure or crystallization kinetics that may lead to the differences in mechanical properties. In an earlier study on this issue,[16] we have shown that incorporation of PN to PP does not influence crystallization dynamics, but in the presence of $CaCO_3$, apart from the five distinct crystalline peaks of α-form of PP, a new peak at 2θ ~15.98° corresponding to the (300) crystal plane of β-form was observed. However, as this change is irrespective of the presence of PN or its content, we can corroborate the above-concluded statement that PN is independently contributing to the notched impact strength of the systems.

3.3. Deformation Mechanisms during Tensile Straining. When the PP/PN blend was unloaded before reaching the tensile yield stress (at maximum load), only the pre-existent submicrometer voids were observed and no other deformation features were evident (and so the micrograph is not shown here). But when the sample was subjected to an

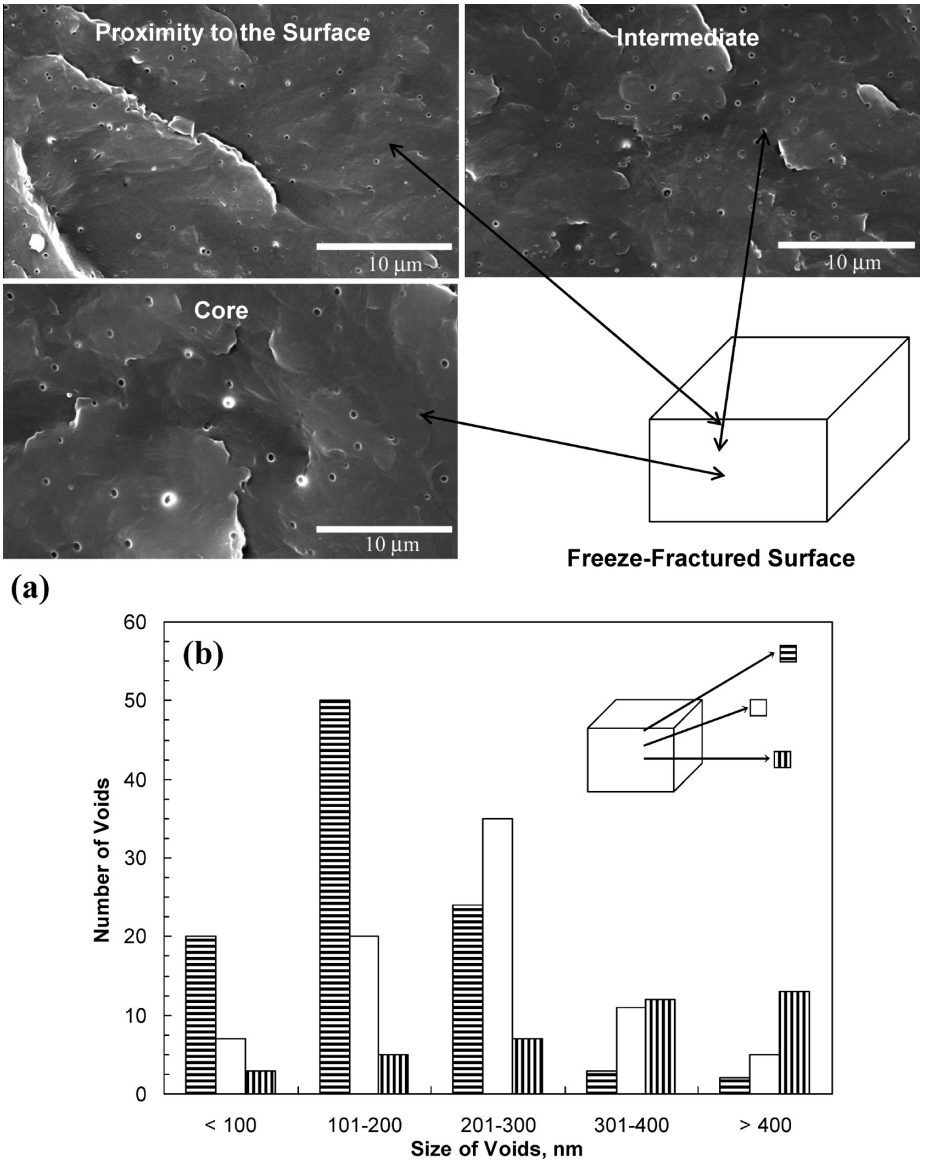

Figure 1. (a) SEM micrographs of the freeze-fractured surfaces of PP/PN blend in the core, intermediate, and proximity to the surface at a selected PN content of 1.5 phr and (b) size distributions of voids in the corresponding regions.

Table 1. Average Size of Submicrometer Voids and Their Number Density in Different Regions of Injection-Molded PP with Varying PN Content and PP/PN/$CaCO_3$ with 1.5 phr PN and 15 wt % $CaCO_3$

	mean void size (nm)			number density of voids (μm^{-2})		
specimen	surface	intermediate	core	surface	intermediate	core
PP/PN (0.75 phr)	200	290	315	0.10	0.048	0.033
PP/PN (1.50 phr)	280	310	350	0.16	0.11	0.06
PP/PN (2.25 phr)	340	380	620	0.16	0.12	0.08
PP with 1.5 phr PN and 15 wt % $CaCO_3$	315	360	545	0.10	0.06	0.04

extension corresponding to the tensile yield stress (~20%), some extent of (plastic) growth of the pre-existent voids was observed, which subsequently seemed to be involved in the process of crazing. Of course, crazing is an energy absorption mechanism and also a cause for the failure of polymers. Previous studies on crazing in various polymers have suggested that the growth of crazes occurs by a process that involves existing voids advancing fingerlike extensions into the bulk polymer and linking up the stretched fibrils in their wake.[17−19] That is, a continuous void network develops between the two craze interfaces with fibril "pillars" (the entangled materials between the void networks are plastically stretched and transformed into fibrils). This leads to the formation of craze tufts or domainlike structure of crazes. A TEM micrograph exemplifying this behavior is shown in Figure 4a.

When the blend was stretched to an extension of 50% (where a neck was observed), the local stress intensification within the craze increased, causing an increase in the number of fibrils to snap, thereby, enlarging the void content (Figure 4b). Finally, the breakdown of craze structure took place by this coalescence of voids. Also, because of distributed voids, crazes were observed to nucleate and grow randomly, depending on the stress states in those regions.

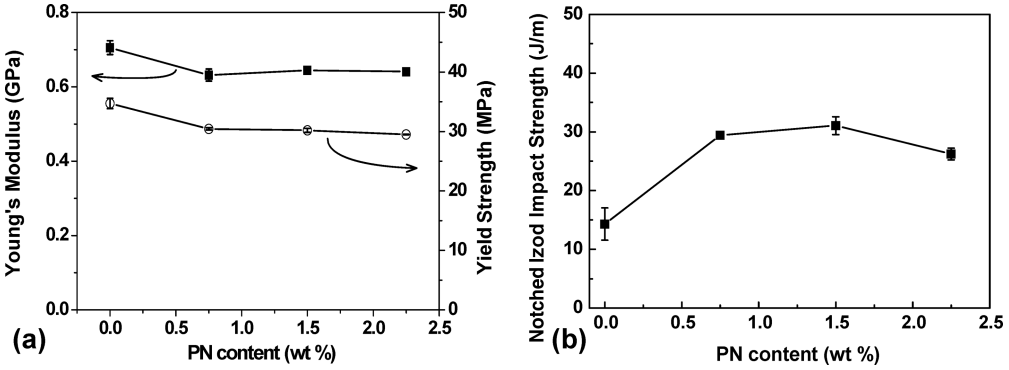

Figure 2. Influence of the presence of PN at different amounts (0.75, 1.50, and 2.25 phr) in PP on (a) Young's modulus and yield strength and (b) notched Izod impact strength of PP/PN blends.

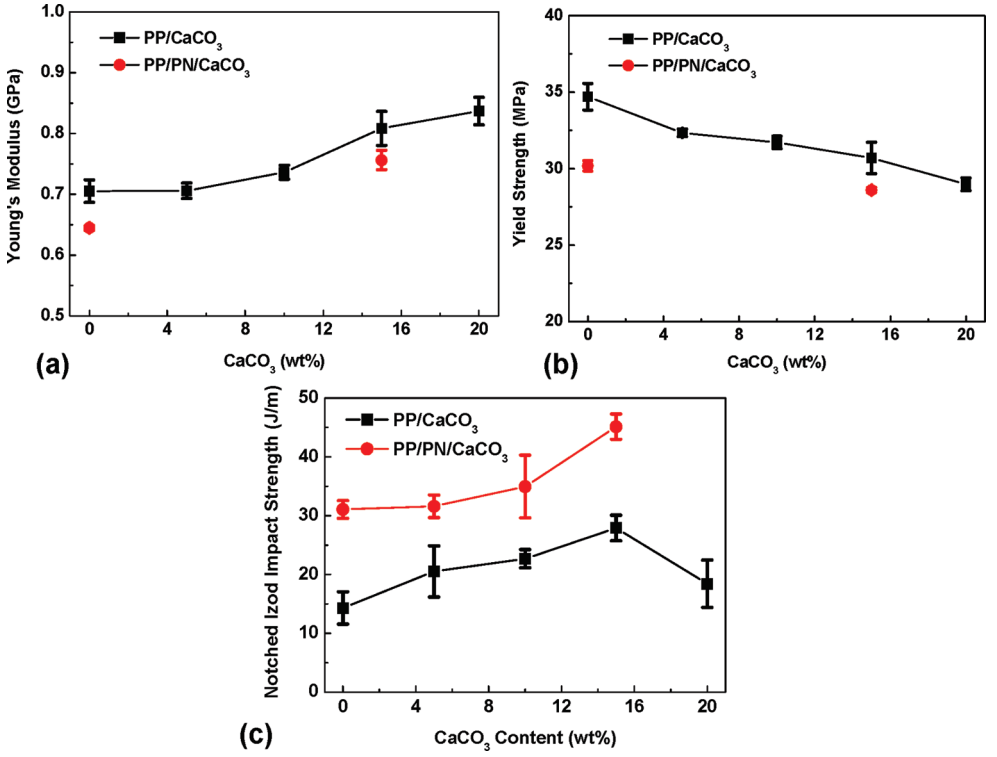

Figure 3. Influence of adding $CaCO_3$ particles to PP with and without PN (1.50 phr) on (a) Young's modulus, (b) yield strength, and (c) notched Izod impact strength of the composites.

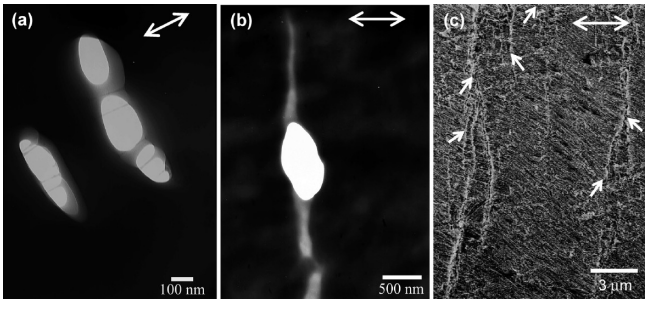

Figure 4. TEM (a, b) and SEM (c) micrographs of PP/PN blend at 1.50 phr PN taken along a plane parallel to the tensile direction unloaded at different extensions showing (a) the formation of domainlike structure of crazes, (b) breakdown of the craze structure and coalescence of the voids, and (c) well-propagated crazes. Tensile direction is shown with double-headed arrows, and single-headed arrows in (c) point to the branching of crazes.

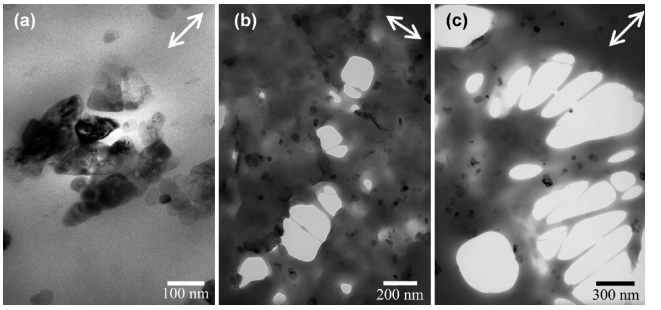

Figure 5. TEM micrographs of PP/$CaCO_3$ composite taken along a plane parallel to the tensile direction from midthickness regions unloaded at (a) tensile yield stress and (b, c) 50% extension. Tensile direction is shown with double-headed arrows.

On a broader scale, to confirm this behavior, *in situ* tensile testing in an SEM chamber was performed. To localize the deformation and focus only at the selected region, a blunt notch was introduced in the sample. At 50% extension, the observations revealed well-propagated craze structures from those originated at the notch (Figure 4c). At similar test

conditions, the magnitude of crazing was small in neat PP. This indicates the effectiveness of the presence of distributed voids in the system. DN-4-PB tests also confirm these observations (see section 3.4).

For the PP/$CaCO_3$ system at 15 wt % of $CaCO_3$ and in the absence of PN, TEM micrographs taken upon unloading to two different extensions are shown in Figures 5a and 5b,c. The large aggregates act as stress concentration sites and result in debonding of loosely held particles from the agglomerates (Figure 5a). It has been suggested that, in principle, debonding/voiding at the particle−polymer interface is required to activate tough response in the surrounding polymer matrix by altering the stress state; hence, strong adhesion and interaction between particles and matrix are not always conducive to toughening.[16,20−23] For example, Thio et al.[22] studied the influence of interfacial strength between PP and surface-modified glass particles on fracture toughness of the composites. They functionalized glass particles with two different silane molecules: *n*-decyltrichlorosilane (with a hydrocarbon end group) to promote adhesion between particles and matrix and heptadecafluorodecyl trichlorosilane (with a fluorocarbon end group) to weaken the adhesion. As expected, the results obtained from tensile dilatometry and mechanical tests showed the weaker adhesion between rigid filler particles and polymer yields earlier and more prevalent debonding that ultimately translates into higher macroscopic toughness. This was also reiterated in our previous investigation on polyamide 6/clay nanocomposites;[24] it was concluded that in the same way as rubber cavitation is a necessary condition for matrix shear yielding to impart high toughness to the polymer/rubber blends, debonding at the polymer/clay interface is an essential factor for *effective* toughening of polymer/clay nanocomposites. In the present study, full scale debonding of $CaCO_3$ particles occurs and alters the stress state in the surrounding material and triggers plastic deformation by the crazing mechanism. The debonding of the particles also enables plastic void growth in the PP matrix. This has been reported for other polymer composite systems in refs 25−28. On further stretching, large-scale debonding occurs, and crazes are formed in a manner similar to PP/PN. However, in this case, due to the nonuniformity in the debonding nature, isolated crazes are formed (Figure 5b,c). Nonetheless, it appears

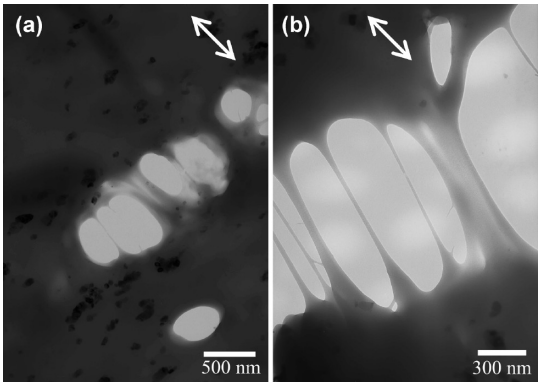

Figure 6. Representative TEM micrographs of PP/PN/$CaCO_3$ nanocomposite taken along a plane parallel to the tensile direction from midthickness regions unloaded at a selected extension of 50%, showing the formation of isolated craze structures of different sizes in different locations. Tensile direction is shown with double-headed arrows.

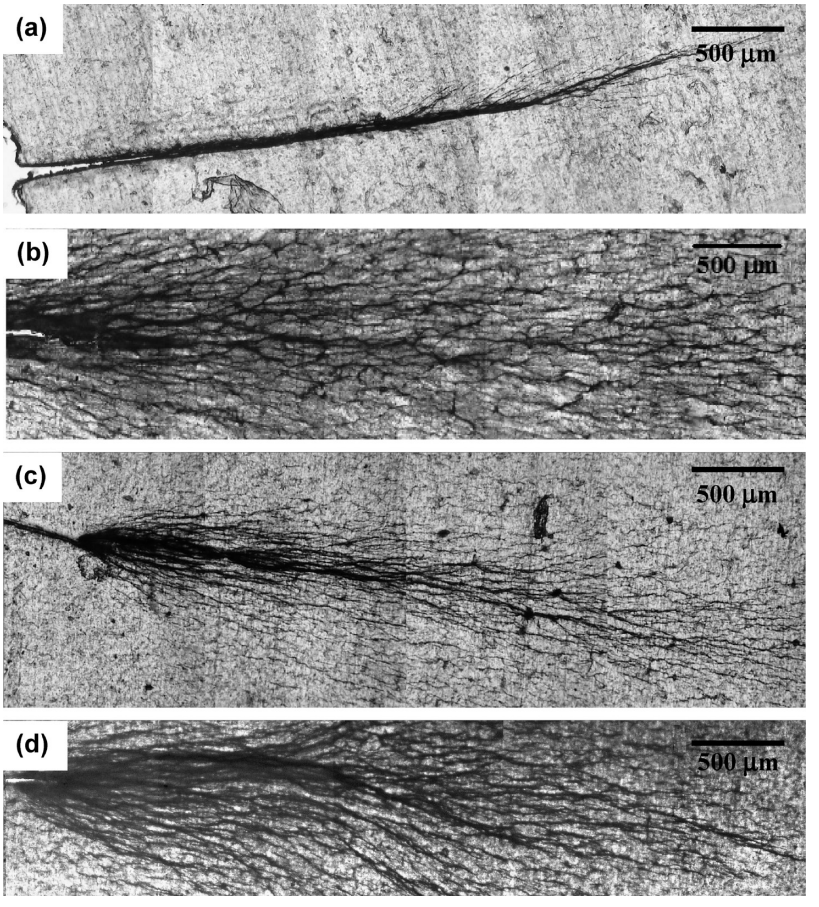

Figure 7. Bright field TOM photographs of (a) PP, (b) PP/PN blend (1.5 phr PN), (c) PP/$CaCO_3$ composite (15 wt % $CaCO_3$), and (d) PP/PN/$CaCO_3$ (1.5 phr PN and 15 wt % $CaCO_3$) nanocomposite from the damage zone of the unbroken notch of the DN-4-PB tests.

that debonding is necessary to enhance the toughness of the system.

The mechanisms involved in the PP/PN/$CaCO_3$ system are interesting, as they are a direct reflection of the combined deformation mechanisms of PP/PN and PP/$CaCO_3$ systems resulting in enhanced notched impact strength. When the sample was subjected to an extension corresponding to the tensile yield stress, voids associated with the debonding of some agglomerated structures of $CaCO_3$ particles were noticed analogous to the PP/$CaCO_3$ system, and some pre-existent voids were involved in the crazing process similar to the PP/PN system. However, in PP/PN/$CaCO_3$ system, because of better dispersion of $CaCO_3$ particles in the PP matrix, the extent of debonding is less when compared to the PP/$CaCO_3$ system without PN. Representative TEM micrographs at a selected extension of 50% and taken at two locations illustrate the domainlike structure of crazes of different sizes (Figure 6).

Therefore, the significant increase in notched impact strength of the ternary material system was attributed to a combination of the processes that happened in the binary blend and binary nanocomposite; that is, the energy dissipated by debonding of the $CaCO_3$ particles and, more significantly, the energies associated with plastic void growth in PP matrix based on both pre-existent voids and those created from particle debonding, as well as void coalescence.

3.4. Deformation Mechanisms during DN-4PB Test. TOM micrographs from the subcritical damage zone of the unbroken notches of PP, PP/PN, PP/$CaCO_3$, and PP/PN/$CaCO_3$ are shown in Figure 7. A typical similar craze pattern is revealed in all cases, though the magnitude of crazing is very high in materials with PN. Indeed, the size of the damage (craze) zone scales with the impact strength results. Also, consistent with the *in situ* tensile straining experiments, the craze patterns in these systems show similarly well-propagated branches. Further, TEM investigations also revealed that the mechanisms involved are similar to tensile deformation mechanisms. So, to avoid repetitions, the micrographs are not shown here.

In summary, this study shows an alternative and effective approach to improve the impact strength of polymers, albeit only 2−3 times. In rubber-toughened systems, however, the improvement can be 7−10 times but with significant losses in both elastic modulus and strength. It would, therefore, be interesting to design and fabricate materials having submicrometer and nanosized voids with an additional presence of minor quantities of dispersed elastomer particles where a synergism in toughness improvement can be expected and, at the same time, drastic losses in stiffness/strength avoided.

4. Conclusions

(1) A nonionic modifier (PN) was used in minor amounts to obtain well-distributed submicrometer to nanosized voids in PP and PP/$CaCO_3$ nanocomposites.

(2) Young's modulus and yield strength of PP (or PP/$CaCO_3$) in the presence of PN were relatively unaffected, but the notched Izod impact strength of the materials was significantly increased.

(3) Detailed investigations of the plastic damage occurring in the tensile and DN-4-PB tests of PP/PN revealed that the voids acted similar to cavitated rubber particles where plastic growth (of the pre-existent voids) in the PP matrix occurred upon deformation and subsequently resulted in the formation of isolated and domainlike structure of crazes.

(4) In the absence of PN, submicrometer voids associated with the debonding of loosely bound $CaCO_3$ particles occurred and subsequently led to the formation of crazes.

(5) PP/PN/$CaCO_3$ system exhibited a combination of the processes that occurred in PP/PN and PP/$CaCO_3$ systems, resulting in significant increase in the notched impact strength.

Acknowledgment. The authors thank the Australian Research Council (ARC) for the financial support of this work which is part of the larger project on "Polymer Nanocomposites".

References and Notes

(1) Bartczak, Z.; Argon, A. S.; Cohen, R. E.; Weinberg, M. *Polymer* **1999**, *40*, 2347–2365.
(2) Chan, C. M.; Wu, J. S.; Li, J. X.; Cheung, Y. K. *Polymer* **2002**, *43*, 2981–2992.
(3) Shah, D.; Maiti, P.; Gunn, E.; Schmidt, D. F.; Jiang, D. D.; Batt, C. A.; Giannelis, E. P. *Adv. Mater.* **2004**, *16*, 1173–1177.
(4) Zuiderduin, W. C. J.; Westzaan, C.; Huetink, J.; Gaymans, R. J. *Polymer* **2003**, *44*, 261–275.
(5) Bagheri, R.; Pearson, R. A. *Polymer* **1996**, *37*, 4529–4538.
(6) Bagheri, R.; Pearson, R. A. *Polymer* **1995**, *36*, 4883–4885.
(7) Bagheri, R.; Pearson, R. A. *Polymer* **2000**, *41*, 269–276.
(8) Danielsson, M.; Parks, D. M.; Boyce, M. C. *J. Mech. Phys. Solids* **2002**, *50*, 351–379.
(9) Guild, F. J.; Young, R. J. *J. Mater. Sci.* **1989**, *24*, 2454–2460.
(10) Fukui, T.; Kikuchi, Y.; Inoue, T. *Polymer* **1991**, *32*, 2367–2371.
(11) Lazzeri, A.; Bucknall, C. B. *J. Mater. Sci.* **1993**, *28*, 6799–6808.
(12) Huang, Y.; Kinloch, A. J. *Polymer* **1992**, *33*, 1330–1332.
(13) Dasari, A.; Yu, Z. Z.; Mai, Y.-W. *Polymer* **2005**, *46*, 5986–5991.
(14) Bartczak, Z.; Argon, A. S.; Cohen, R. E.; Weinberg, M. *Polymer* **1999**, *40*, 2331–2346.
(15) Zhang, Y.; Chan, C. M.; Wu, J. S. ANTEC, Chicago, **2004**; p 1795.
(16) Zhang, Q. X.; Yu, Z. Z.; Xie, X. L.; Mai, Y.-W. *Polymer* **2004**, *45*, 5985–5994.
(17) Argon, A. S.; Cohen, R. E. *Mater. Sci. Eng.* **1994**, *A176*, 79–90.
(18) Young, R. J.; Lowell, P. A. In *Introduction to Polymers*, 2nd ed.; Chapman & Hall: London, 1991; p 177.
(19) Rabinowitz, S.; Beardmore, P. *CRC Crit. Rev. Macromol. Sci.* **1972**, *1*, 1–5.
(20) Lazzeri, A.; Zebarjad, S. M.; Pracella, M.; Cavalier, K.; Rosa, R. *Polymer* **2005**, *46*, 827–844.
(21) Thio, Y. S.; Argon, A. S.; Cohen, R. E.; Weinberg, M. *Polymer* **2002**, *43*, 3661–3674.
(22) Thio, Y. S.; Argon, A. S.; Cohen, R. E. *Polymer* **2004**, *45*, 3139–3147.
(23) Lazzeri, A.; Thio, Y. S.; Cohen, R. E. *J. Appl. Polym. Sci.* **2004**, *91*, 925–935.
(24) Dasari, A.; Yu, Z. Z.; Mai, Y.-W. *Macromolecules* **2007**, *40*, 123–130.
(25) Johnsen, B. B.; Kinloch, A. J.; Mohammed, R. D.; Taylor, A. C.; Sprenger, S. *Polymer* **2007**, *48*, 530–541.
(26) Johnsen, B. B.; Kinloch, A. J.; Taylor, A. C. *Polymer* **2005**, *46*, 7352–7369.
(27) Tzika, P. A.; Boyce, M. C.; Parks, D. M. *J. Mech. Phys. Solids* **2000**, *48*, 1893–1929.
(28) Steenbrink, A. C.; Van der Giessen, E.; Wu, P. D. *J. Mater. Sci.* **1998**, *33*, 3163–3175.